

Machine-learning identification of galaxies in the WISE × SuperCOSMOS all-sky catalogue

T. Krakowski¹, K. Małek^{1,2}, M. Bilicki^{3,2}, A. Pollo^{1,4,2}, M. Krupa^{4,2}, A. Kurcz^{4,2}

¹ National Centre for Nuclear Research, ul. Andrzeja Sołtana 7, 05-400 Otwock, Poland e-mail: tomasz.krakowski@ncbj.gov.pl

² Janusz Gil Institute of Astronomy, University of Zielona Góra, ul. Lubuska 2, 65-265 Zielona Góra, Poland

³ Leiden Observatory, Leiden University, P.O. Box 9513 NL-2300 RA Leiden, The Netherlands

⁴ Astronomical Observatory of the Jagiellonian University, ul. Orla 171, 30-244 Kraków, Poland

April 20, 2022

ABSTRACT

Context. The two currently largest all-sky photometric datasets, WISE and SuperCOSMOS, were cross-matched by Bilicki et al. (2016) (hereafter B16) to construct a novel photometric redshift catalogue on 70% of the sky. Galaxies were therein separated from stars and quasars through colour cuts, which may leave imperfections because of mixing different source types which overlap in colour space.

Aims. The aim of the present work is to identify galaxies in the WISE × SuperCOSMOS catalogue through an alternative approach of machine learning. This allows us to define more complex separations in the multi-colour space than possible with simple colour cuts, and should provide more reliable source classification.

Methods. For the automatised classification we use the support vector machines (SVM) learning algorithm, employing SDSS spectroscopic sources cross-matched with WISE × SuperCOSMOS as the training and verification set. We perform a number of tests to examine the behaviour of the classifier (completeness, purity and accuracy) as a function of source apparent magnitude and Galactic latitude. We then apply the classifier to the full-sky data and analyse the resulting catalogue of candidate galaxies. We also compare thus produced dataset with the one presented in B16.

Results. The tests indicate very high accuracy, completeness and purity (> 95%) of the classifier at the bright end, deteriorating for the faintest sources, but still retaining acceptable levels of ~ 85%. No significant variation of classification quality with Galactic latitude is observed. Application of the classifier to all-sky WISE × SuperCOSMOS data gives 15 million galaxies after masking problematic areas. The resulting sample is purer than the one in B16, at a price of lower completeness over the sky.

Conclusions. The automatic classification gives a successful alternative approach to defining a reliable galaxy sample as compared to colour cuts. Thus obtained identifications will be included in the public release of the WISE × SuperCOSMOS galaxy catalogue available from <http://ssa.roe.ac.uk/WISExSCOS>.

Key words. Methods: data analysis, numerical – Astronomical databases: miscellaneous – Galaxies: statistics – Cosmology: large-scale structure of Universe

1. Introduction

Modern wide-field astronomical surveys include millions of sources, and the forthcoming ones will raise these numbers to billions. As most of the detected objects cannot be followed up spectroscopically, research done with such datasets will heavily rely on photometric information. Unavailability of spectroscopy however complicates appropriate identification of various source types, usually possible with high reliability only if spectra are available. In the seemingly most trivial case of star-galaxy separation in deep imaging catalogues, one quickly reaches the limit where this cannot be done based on morphology: due to resolution limitations, distant, faint galaxies become unresolved – point-like – as stars (e.g. Vasconcellos et al. 2011). Additional information is then needed to separate out these and sometimes other (such as point-like but extragalactic quasars) classes of sources. This has been traditionally done with magnitude and colour cuts; however, when the parameter space is multi-dimensional, such cuts become very complicated. Additionally, noise in photometry scatters sources from their true positions in the colour space. This, together with huge numbers of sources, most of which are usually close to the survey’s detection limit,

precludes reliable overall identification with any manual – or ‘eye-balling’ – methods. For these reasons, the idea of automatized source classification has recently gained on popularity, and was applied to such multi-wavelength datasets as, for instance, AKARI (Solarz et al. 2012), Panoramic Survey Telescope and Rapid Response System (Pan-STARRS, Saglia et al. 2012), VIMOS Public Extragalactic Redshift Survey (VIPERS, Małek et al. 2013), Wide-field Infrared Survey Explorer – Two Micron All Sky Survey (WISE–2MASS) cross-match (Kovács & Szapudi 2015), Sloan Digital Sky Survey (SDSS, Brescia et al. 2015), WISE-only (Kurcz et al. 2016), as well as tested in view of the Dark Energy Survey data (Soumagnac et al. 2015).

The present paper describes an application of a machine learning algorithm to identify galaxies in a newly compiled dataset, based on two presently the largest all-sky photometric catalogues: WISE in the mid-infrared and SuperCOSMOS in the optical. This work is a refinement of a simpler approach to source classification applied in Bilicki et al. (2016), hereafter B16, where stars and quasars were filtered out on a statistical basis using colour cuts to obtain a clean galaxy sample for the purpose of photometric redshift calculation. The two parent catalogues we use here, described in detail hereunder and in Sec. 2,

both include of the order of a billion detections, of which a large part are common. For various reasons, however, the available data products from these two surveys offer limited information on the nature of the catalogued objects, which indeed presents a challenge to the classification task.

WISE (Wright et al. 2010), being more sensitive of the two, suffers from low native angular resolution resulting from the small aperture of the telescope (40 cm): it is equal to $6.1''$ in its shortest $W1$ band ($3.4 \mu\text{m}$), rising to $12''$ at the longest-wavelength $W4$ of $23 \mu\text{m}$. This leads to severe blending in crowded fields, such as at low Galactic latitudes, and original photometric properties of the blended sources become mixed. In addition, proper isophotal photometry has not been performed for the majority of WISE detections and no WISE all-sky extended source catalogue is yet available (see however Cluver et al. 2014 and Jarrett et al. 2016 for descriptions of ongoing efforts to improve on this situation). Finally, WISE-based colours provide limited information for classification purposes: at rest frame, the light in its two most sensitive passbands, $W1$ and $W2$ (3.4 and $4.6 \mu\text{m}$), is emitted from the photospheres of evolved stars (Rayleigh-Jeans tail of the spectrum) and the catalogue is dominated by stars and relatively low-redshift galaxies, which usually have similar $W1 - W2$ colours. The two other WISE filters, $W3$ and $W4$ centred respectively at 12 and $23 \mu\text{m}$, which could in principle serve to reliably separate out stars from galaxies and QSOs when combined with $W1$ and $W2$ (Wright et al. 2010), offer far too low detection rates to be applicable for most of the WISE sources.

SuperCOSMOS (hereafter SCOS) on the other hand, based on the scans of twentieth century photographic plates (Hambly et al. 2001c), does offer point and resolved source identification (Hambly et al. 2001b). This classification, although quite sophisticated, is however based mostly on morphological information, and on the one hand, unresolved galaxies and quasars are classified as point sources, and on the other, blending in crowded fields (Galactic Plane and Bulge, Magellanic Clouds) leads to spurious ‘extended’ source identifications (see also Peacock et al. 2016).

A cross-match of the WISE and SCOS catalogues improves the classification of different types of sources useful for extragalactic applications, as shown in B16. Still however, although only *extended* SCOS sources were considered therein, blends mimicking resolved objects dominated at Galactic latitudes as high as $\pm 30^\circ$ and had to be removed on a statistical basis. In the present paper we move one step further in view of generating a wide-angle (almost full sky) galaxy catalogue from the WISE \times SCOS cross-match. For this purpose we use the Support Vector Machines (SVM) supervised machine learning algorithm.

A similar task for other WISE-based datasets was undertaken in two recent works. Kovács & Szapudi (2015), used a cross-match of WISE $W1 < 15.2$ sources with the 2MASS Point Source Catalogue (PSC, Skrutskie et al. 2006) and having performed an SVM analysis in multicolour space, showed that a cut in the $W1_{\text{WISE}} - J_{2\text{MASS}}$ colour gives efficient star/galaxy separation. Based on these results, they produced a galaxy catalogue containing 2.4 million objects with estimated star contamination of 1.2%, and galaxy completeness of 70%. The separation was made for stars and galaxies only, with no information regarding quasars. A limitation of a WISE – 2MASS cross-match is a much smaller depth of the latter with respect to the former. Most of 2MASS galaxies are located within $z < 0.2$ (Bilicki et al. 2014; Rahman et al. 2016), while WISE extends well beyond that, detecting L_* galaxies at $z \sim 0.5$ (Jarrett et al. 2016).

Using photometric information only from WISE, in Kurcz et al. (2016) our team employed SVM and attempted at classi-

fying all unconfused WISE sources brighter than $W1 < 16$ into 3 classes: stars, galaxies, and quasars. This led to identification of 220 million candidate stars, 45 million candidate galaxies and 6 million candidate QSOs. The latter sample is however significantly contaminated with what we interpret as a possibly very local foreground, such as asteroids or zodiacal light.

The present paper is laid out as follows: the description of the data can be found in Section 2; Section 3 describes the principles of the Support Vector Machine learning algorithm and introduces the training sample used in our work; in Section 4 we present various tests which allowed us to quantify the performance of the SVM algorithm. Section 5 contains the description and properties of the final galaxy catalogue, as well as a comparison with B16 results. In Section 6 we present a summary of our analysis.

2. Data: WISE and SuperCOSMOS

The catalogues used to construct the main photometric dataset, WISE and SuperCOSMOS, are comprehensively described in Bilicki et al. (2014) and B16. Here we briefly summarize them and the preselections applied for the purpose of this project. They are practically equivalent to those from the latter paper; for more details see section 2 of B16, and in particular table 1 and figs. 1–3 therein.

2.1. WISE

The Wide-field Infrared Survey Explorer (WISE; Wright et al. 2010), a NASA space-based mission, surveyed the entire sky in four mid-infrared (IR) bands: 3.4 , 4.6 , 12 and $23 \mu\text{m}$ ($W1 - W4$ respectively). Here we use its second full-sky release, the All-WISE dataset¹ (Cutri et al. 2013), combining data from the cryogenic and post-cryogenic survey phases. It includes almost 750 million sources with signal-to-noise (S/N) ratio ≥ 5 in at least one of the bands, and its averaged 95% completeness in unconfused areas is $W1 \lesssim 17.1$, $W2 \lesssim 15.7$, $W3 \lesssim 11.5$ and $W4 \lesssim 7.7$ in Vega magnitudes, with however variable coverage being the highest at ecliptic poles and the lowest near the ecliptic, especially in stripes resulting from Moon avoidance manoeuvres.

Our WISE preselection required sources with S/N ratios larger than 2 in the $W1$ and $W2$ bands, and not being obvious artefacts (`cc_flags[1,2] \neq ‘DPHO’`); this gives 603 million detections over the whole sky. Due to low survey resolution ($\sim 6''$), the immensely crowded Galactic Plane and Bulge are totally dominated by stellar blends and extracting especially extragalactic information in there is practically impossible (extinction however not being such an issue in the WISE passbands unless in very high-extinction regions). We will thus limit ourselves to the 83% of the sky available at $|b| > 10^\circ$, which reduces the sample to about 460 million objects. Furthermore, for uniformity purposes, we applied a flux limit of $W1 < 17$ which gave a final input WISE dataset of about 343 million sources at $|b| > 10^\circ$. At the bright end this sample is dominated by stars even at high Galactic latitudes (Jarrett et al. 2011; Jarrett et al. 2016) and we estimate about 100 million of the WISE sources, mostly faint, to be galaxies and quasars (B16; Kurcz et al. 2016), the rest being of stellar nature.

WISE database currently does not offer reliable (e.g. isophotal) aperture photometry for the resolved sources and the latter are not even identified therein (except for less than 500,000

¹ Available for download from IRSA at <http://irsa.ipac.caltech.edu>.

cross-matches with the 2MASS Extended Source Catalog). In what follows we thus use the w_{mpro} magnitudes (where ‘?’ stands for the channel number), based on PSF profile-fit measurements. The only proxy for morphological properties that we adopt here from the database is given by circular aperture measurements performed on the sources within a series of fixed radii, obtained however without any contamination removal or missing pixels compensation. In particular, as in Bilicki et al. (2014) and Kurcz et al. (2016), in the classification procedure we will be using a differential measure – or a *concentration parameter* – defined as

$$w_{\text{mag}13} = w_{\text{mag}_1} - w_{\text{mag}_3}, \quad (1)$$

where w_{mag_1} and w_{mag_3} were measured in fixed circular apertures of radii respectively $5.5''$ and $11''$. The $w_{\text{mag}13}$ parameter is expected to have different distributions for point and resolved sources, which indeed is the case as we verified against SDSS spectroscopic data described in Sec. 3.1.

Note that out of the four available WISE bands we will not be employing the longest-wavelength W4 due to its very low sensitivity, leading to an overwhelming number of non-detections. In addition, whenever W3 is used, all the sources with $w_{3\text{snr}} < 2$ (upper limits and non-detections, which together dominate the W3 channel in our sample), will be artificially ‘dimmed’ by $+0.75$ mag to statistically compensate for their overestimated fluxes, which we determined to be an appropriate average correction. Possible errors associated with this procedure will not be however important for our final catalogue, as we will eventually not employ the $12\ \mu\text{m}$ passband for the overall classification, because of the photometry issues, although it does bring some improvement (cf. Sec. 4.1). The W3 information was used only in the test phase.

2.2. SuperCOSMOS

The SuperCOSMOS Sky Survey (SCOS, Hambly et al. 2001a,b,c) consists of digitized photographs in three bands, B, R, I , obtained via automated scanning of source plates from the United Kingdom Schmidt Telescope (UKST) in the South and the Palomar Observatory Sky Survey-II (POSS-II) in the North, the observations having been conducted in the last decades of the twentieth century. The data is publicly available from the SuperCOSMOS Science Archive², with photometric, morphological and quality information for 1.9 billion sources.

SCOS provides source classification flags in each of the three bands, as well as a combined one, meanClass , equal to 1 if source is resolved, 2 if unresolved, 3 if unclassifiable and 4 if probably noise (Hambly et al. 2001b), the two latter comprising a negligible fraction ($\ll 1\%$) of all the sources. The derived catalogue of extended sources was accurately calibrated all-sky using SDSS photometry in the relevant areas, and the calibration was extended over the rest of the sky by matching plate overlaps and by using the average color between the optical and 2MASS J bands (Peacock et al. 2016). This however is not the case for the point sources, which very much limits their applicability for uniform source selection. In B16 only the SCOS sources with $\text{meanClass} = 1$ were used in order to obtain a WISE \times SCOS galaxy sample that was further purified of residual quasars and stars. In the present paper we follow this preselection, reiterating however that only a part of such SCOS sources are in fact extragalactic. Especially at low Galactic latitudes, this extended source catalogue is dominated by blends of

stars with other stars and with extragalactic objects. The remaining SCOS preselections are also the same as in B16 and earlier in Bilicki et al. (2014): objects need to be properly detected with aperture photometry in the B and R bands³ (gCorMagB and gCorMagR2 not null; quality flags qualB and $\text{qualR2} < 2048$, meaning no strong warnings nor severe defects, Hambly et al. 2001b).

The publicly available catalogue was supplemented with additional data in corners of the photographic plates, missing from the original dataset due to so-called ‘step-wedges’ (Hambly et al. 2001b). This affects mostly low declinations. The B and R magnitudes were additionally calibrated between the North and the South (the split being at $\delta_{1950} = 2.5^\circ$) to compensate for differences between effective passbands of UKST and POSS-II; see Peacock et al. (2016) for details.

In order to preserve all-sky photometric reliability and to mitigate issues with catalogue depth varying from plate to plate, two flux limits were applied to the SCOS dataset, $B < 21$ and $R < 19.5$ (AB-like, extinction-corrected). As already mentioned, we have not used the Galactic Plane strip of $|b| < 10^\circ$, where blending and high extinction make SCOS photometry unreliable. The resulting SCOS catalogue of extended sources outside of the Galactic Plane includes over 85 million objects.

2.3. Cross-matched WISE \times SuperCOSMOS photometric sample

The two photometric catalogues were paired up using a matching radius of $2''$. The resulting flux-limited cross-matched sample at $|b| > 10^\circ$ contains almost 48 million sources. This number includes WISE sources supplemented from an earlier, cryogenic phase of observations (‘All-Sky’, Cutri et al. 2012), to fill in strips of missing data centred at ecliptic longitudes of $\lambda \sim 50^\circ$ and $\lambda \sim 235^\circ$.

In what follows, all the magnitudes are extinction-corrected using the Schlegel et al. (1998) maps and applying the following extinction coefficients, derived from the Schlafly & Finkbeiner (2011) re-calibration (B16): $A_B = 3.44$, $A_R = 2.23$, $A_{W1} = 0.169$, and $A_{W2} = 0.130$. The usage of de-reddened magnitudes also for stars is motivated by the fact that we focus on extragalactic sources, the stellar ones being contamination for our applications. As these corrections are often significant in the optical, neglecting them would lead to considerable biases in the final galaxy catalogue. Still, we will not be using the areas of very high extinction, $E(B - V) > 0.25$, where there is practically no training data for classification, and the photometry especially in the optical is problematic. This cut, removing further 7.2 million sources, is the same as applied in B16, where the appropriate threshold was determined through an analysis of spurious under- and overdensities in WISE \times SCOS source distribution.

Figure 1 motivates the usage of an automatic classifier rather than simple colour cuts to separate out galaxies from stars and quasars in the WISE \times SCOS sample. The diagrams illustrate distributions of three source types (galaxies, quasars and stars) on two colour-colour (c - c) planes. Source identifications come from a WISE \times SCOS \times SDSS cross-match described in details in Sec. 3.1. In the left panel we show the $W2 - W3$ vs. $W1 - W2$ c - c plane, which is often used for object discrimination in WISE (e.g. Jarrett et al. 2011; Ferraro et al. 2015). The plot demonstrates that it is challenging to find simple cuts in these parameters that would maximise both the completeness and the purity of the resulting samples. While one could quite well separate

² <http://surveys.roe.ac.uk/ssa/>

³ We do not use the third SCOS band, I , as it is too shallow.

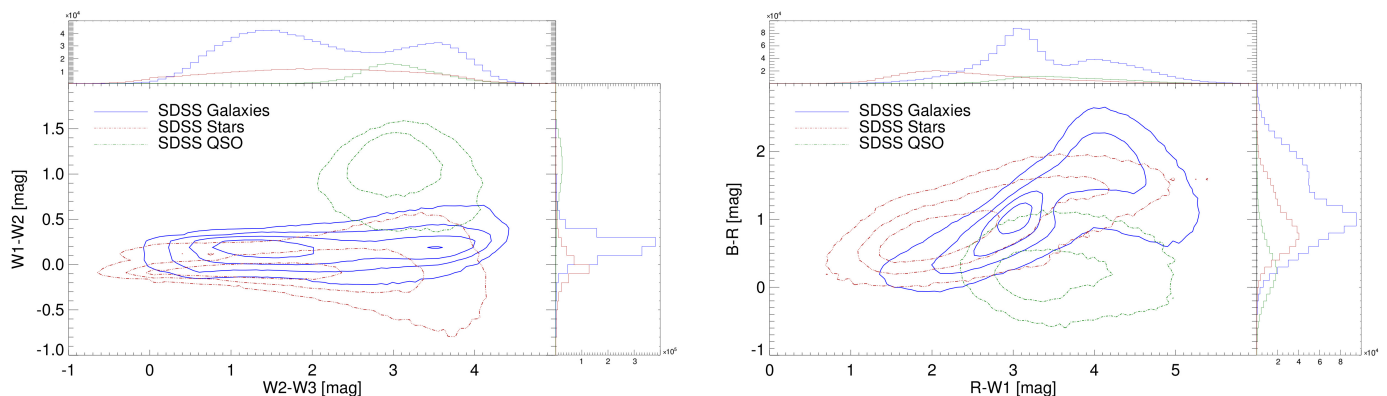


Fig. 1: Colour-colour diagrams for galaxies, stars and quasars from a cross-match of WISE \times SuperCOSMOS with SDSS spectroscopic data. *Left panel:* WISE colours only; *right panel:* WISE and SCOS colors. Blue contours corresponds to galaxies, red contours represent stars, and green contours illustrate quasars.

QSOs from other sources, for example via a $W1 - W2 = 0.8$ cut (Stern et al. 2012; Assef et al. 2013; Yan et al. 2013), it is much more difficult, if at all possible, to apply a single threshold to efficiently separate galaxies from stars. The galaxy and star distributions very much overlap even if the additional colour $W2 - W3$ is taken into account. The situation is similar for other colour combinations available from the five bands in WISE \times SCOS. The right panel of Fig. 1 illustrates the $R - W1$ vs. $B - R$ c-c plane, where also the three source types largely overlap.

3. Classification method: Support Vector Machines

For the classification performed in this work we used the Support Vector Machines (SVM) methodology. SVM is a supervised learning algorithm which is a maximum-margin classifier able to determine decision planes between sets of objects having different class memberships, to find a decision boundary by maximising the margin between the closest points of the classes (the so-called support vectors). Each single object is classified based on its relative position in the n -dimensional parameter space (Cristianini & Shawe-Taylor 2000; Shawe-Taylor & Cristianini 2004; Solarz et al. 2012; Małek et al. 2013).

The SVM algorithm is an increasingly popular way of dealing with astronomical data to classify different types of objects. For various applications of SVM in astronomy we refer the reader to, for instance, Woźniak et al. (2004); Huertas-Company et al. (2008); Solarz et al. (2012); Saglia et al. (2012); Małek et al. (2013); Kovács & Szapudi (2015), Marton et al. (2016), and Kurcz et al. (2016).

In our case, SVM was used to build a non-linear classifier for the photometric data in the WISE \times SCOS all-sky catalogue. As input data we used photometric information such as magnitudes, colours, and a differential aperture magnitude (see Sec. 4 for details). The input data are transformed by a *kernel* into a higher-dimensional feature space, where the separation between different classes is less complex than in the input parameter space. For more details see e.g. Manning et al. (2008) or Małek et al. (2013); an illustrative description of how SVM classification operates is provided in Han et al. (2016). The classifier is trained using a subset of input data for which class identifications are known. In our case, the training set was derived from SDSS DR12 spectroscopic data matched with WISE \times SCOS (see Sec. 3.1).

For our particular implementation, we used a C-SVM algorithm with a Gaussian kernel

to identify three different classes of objects: galaxies, quasars, and stars, with the final aim to reliably pinpoint the galaxies. The Gaussian kernel function (dubbed also radial basic) is defined as

$$k(x_i, y_j) = \exp(-\gamma \|x_i - x_j\|^2), \quad (2)$$

where $\|x_i - x_j\|$ is the Euclidean distance between feature vectors in the input space. The parameters γ and C allow to construct hyperplanes in the multidimensional space that separate cases of different class labels. In particular, they have the following roles:

- * γ is related to the breadth of the Gaussian distribution, σ , namely $\gamma = 1/(2\sigma^2)$, and determines the topology of the decision surface. Too high a value of γ sets a complicated decision boundary, while too low γ can give a decision surface that is too simple, which might cause misclassifications;
- * C is a trade-off parameter, whose large value corresponds to a small margin of separation between different classes of objects, which may cause over-fitting, however too small a value of C can allow for misclassifications.

Both parameters, C and γ , were optimized based on the training set, through a grid search and N -fold cross-validation; we used $N = 10$, in which case the training data are split into 10 equals sets, and the classifier is trained on 9 of them. Then the classifier is tested against the remaining 10th subset (the so-called *self-check* or validation). This test is repeated ten times, with a different subset removed for each training run. The classification accuracy is then calculated by averaging over the ten runs. The same method was used in Solarz et al. (2012) and Małek et al. (2013), where the reader can find a more detailed description of this process. Moreover, one can use an additional *test sample* (data with known classification, but not used for training) for an independent check of the performance of the classifier.

In the test phase of our study, we used only the discrete classes assigned by SVM to each source. For the final classification, however, we decided to employ the full probability distributions for each class. This allowed us to examine the cases of problematic classification where the probabilities that a source belongs to two or three classes were roughly equal. More discussion on this will be provided in Sec. 5.

For our analysis we used LIBSVM6 (Chang & Lin 2011), an integrated software for support vector classification, which

allows for multiclass identifications. We also employed R, a free software environment for statistical computing and graphics, with the e1071 interface (Meyer 2001) package installed.

3.1. Training sample: SDSS DR12 spectroscopic data

A well-chosen training sample is crucial for the SVM method, because the classifier is tuned based on the properties of this sample: the C and γ parameters are estimated and the hyperplane between classes is determined. This means that a representative sample of sources, with already known properties that we want to identify, is essential. In our specific case of a catalogue including $z \lesssim 0.5$ galaxies (Bilicki et al. 2014, B16), as well as stars and higher-redshift quasars, such a training set requires good-quality and high-reliability pre-classification using spectroscopic measurements. For that reason, for training and testing purposes, we chose to employ the spectroscopic sample from the Sloan Digital Sky Survey Data Release 12 (SDSS DR12, Alam et al. 2015) cross-matched with the WISE × SCOS dataset defined above.

The SDSS is a multi-filter imaging and spectroscopic survey, and its DR12, used for our analysis, includes dedicated star, galaxy and quasar surveys. These samples are shallower than the imaging part of the SDSS, they however are available with high reliability only from spectra (Bolton et al. 2012): photometric classification of SDSS was based only on source morphology (resolved vs. point-like, Stoughton et al. 2002). SDSS DR12 contains almost 3.9 million spectroscopic sources, of which 61% were identified as galaxies, 22% as stars and the remaining 16% as quasars/AGNs (SDSS class ‘QSO’). As a quality determinant, to avoid unreliable spectroscopic measurements and hence problematic classification, we applied redshift quality information from the SDSS database: the `zWarning` flag and the relative error in redshift (radial velocity for stars) defined as $\Delta z = z_{\text{err}}/z$, where z_{err} is the database value. In what follows only the sources with `zWarning` = 0 were used, with the additional conditions of $\Delta z < 0.1$ for galaxies and quasars, and $\Delta z < 1$ for stars.

Pairing up these sources with our WISE × SCOS flux-limited catalogue within 1'' matching radius gave over 1 million common objects, of which 95% were galaxies, 2% stars and 3% quasars. Clearly, the stars and most of the quasars are point sources and should not be resolved. The fact that we identify over 50,000 of them in the cross-match of SDSS with the WISE × SCOS extended source catalogue reflects the susceptibility of SCOS morphological classification (the `meanClass` flag) to blending which mimics resolved sources (B16). The main purpose of the present study is to reliably filter out such sources from the galaxy catalogue we aim to produce.

4. SVM classification performance

This Section describes various tests made using the SDSS-based training sample, which allowed us to quantify the performance of the SVM algorithm in view of the final classification of the entire catalogue.

In order to check the classification performance, to calculate dependence on different parameters, as well as to perform the final classification, the following procedure was used: (1) as galaxy properties changes with magnitude, each sample (training and test sets, final catalogue) were divided into five $W1$ magnitude bins ($W1 < 13$, $13 \leq W1 < 14$, $14 \leq W1 < 15$, $15 \leq W1 < 16$ and $16 \leq W1 < 17$); (2) five SVM algorithms separately tuned for these bins were used to classify galaxies, stars, and quasars; (3) five SVM outputs were merged and treated

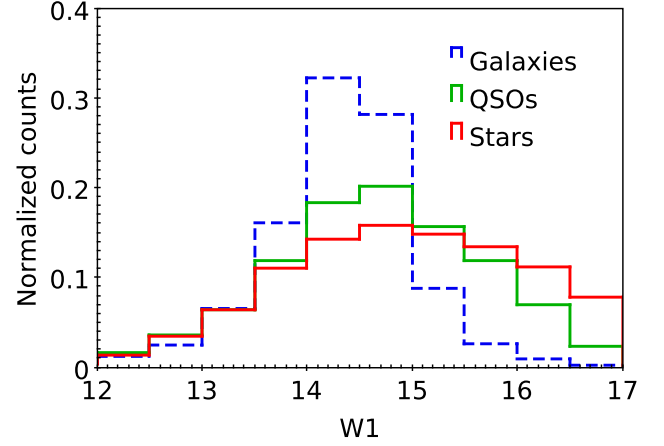


Fig. 2: Normalised number counts of $W1$ magnitudes in the WISE × SCOS × SDSS cross-matched sample for stars, galaxies and quasars.

as one final output. As we checked, there is no evidence for inconsistency between different $W1$ magnitude bins.

Figure 2 shows normalized $W1$ magnitude distributions for the three types of sources in the WISE × SCOS × SDSS cross-match. As was shown in Kurcz et al. (2016), there is a dependence of derived classification statistics on the number of training objects, but the classifier stabilizes for subsamples of 3000 objects in each class. In our case, however, both at the bright ($W1 < 13$) as well as at the faint end ($W1 > 16$) we do not have large enough numbers of sources to select randomly 3000 objects of each class from the input sets to build the training sample. In particular, we need to use all the stars and quasars from these bins for the training and tests. For this reason, our training samples consist of different numbers of objects in each $W1$ bin: respectively 1000, 4000, 4000, 5000 and 2600 of each type for the $12 < W1 < 13$, $13 < W1 < 14$, $14 < W1 < 15$, $15 < W1 < 16$ and $16 < W1 < 17$ mag bins.

The first step of the tests was to determine for the five $W1$ bins the optimal C and γ parameters, therefore we tuned five different C-SVM classifiers for our purpose. Fig. 3 illustrates an exemplary grid search for one of the classifiers. The colours code the mean misclassification rate for given combinations of γ and C ; the lower the rate, the better the performance of the SVM algorithm. Here the misclassification rate is defined for each magnitude bin as the complement to the total accuracy (TA), the latter being the mean of accuracies A_i for individual validation iterations:

$$TA = \frac{1}{10} \sum_{i=1}^{10} A_i. \quad (3)$$

The accuracy for a given iteration is defined as

$$A_i = \frac{TG + TQ + TS}{TG + TQ + TS + FG + FQ + FS}. \quad (4)$$

The components of this equation are: true galaxies (TG), quasars (TQ) and stars (TS) from the training sample, properly classified as galaxies, quasars, and stars, respectively; and false galaxies (FG), being real quasars or stars misclassified as galaxies, with false quasars (FQ) and false stars (FS) defined in a similar manner.

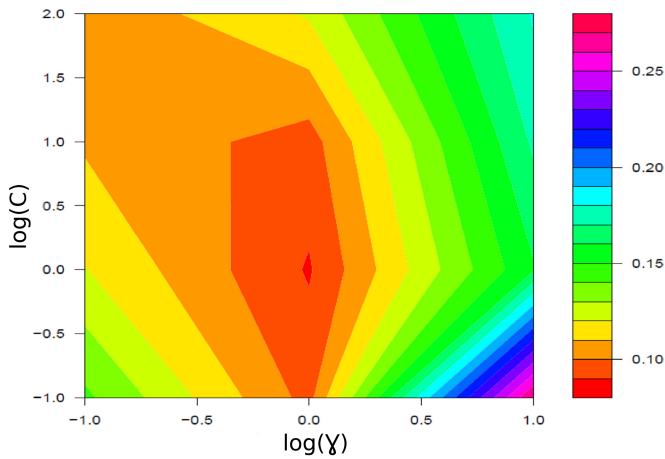


Fig. 3: An example of the $C - \gamma$ plane obtained from one of the five WISE \times SCOS C-SVM classifiers. Mean misclassification rate (colour bar) as a function of the C and γ parameters was estimated through ten-fold cross-validation for each pair of the two parameters. The lower the misclassification rate, the better the performance of the SVM algorithm.

To further compare the performance of different classifiers, we calculated the following measures, as defined by Soumagnac et al. (2015): completeness (c), contamination (f), and purity (p) for galaxy, star, and quasar samples. We used the following equations (here for galaxies):

$$c_g = \frac{\text{TG}}{\text{TG} + \text{FGS} + \text{FGQ}}, \quad (5)$$

$$f_g = \frac{\text{FSG} + \text{FQG}}{\text{TG} + \text{FGS} + \text{FQG}}, \quad (6)$$

$$p_g = 1 - f_g = \frac{\text{TG}}{\text{TG} + \text{FSG} + \text{FQG}}, \quad (7)$$

where FGS and FGQ stand for galaxies mis-classified respectively as stars and quasars, and FSG, FQG are stars and quasars mis-classified as galaxies. Definitions for stars and quasars follow in an analogous way. Accuracy for an individual class of objects is defined in the same way as purity.

4.1. Usefulness of the W3 passband for the classification

We tested two classifiers for the separation between galaxies, quasars, and stars: one with five and the other with six parameters. These were: $W1$ magnitude, $W1 - W2$ colour, $R - W1$ colour, $B - R$ colour, and the $w1\text{mag}13$ differential aperture magnitude for the $W1$ channel. The sixth parameter in the tests was the $W3$ magnitude, often used in WISE-based source classifications (e.g. Kovács & Szapudi 2015; Ferraro et al. 2015), following the considerations of e.g. Wright et al. (2010) that different types of sources occupy different regions of the $W1 - W2$ vs. $W2 - W3$ colour plane. However, as Fig. 1 shows, this idealized picture becomes more complicated for actual observations, and we decided to test how much the $W3$ passband from WISE improves the automatic classification. Note that to avoid biases for overestimated fluxes, a recalibration of the $W3$ upper limits was necessary as discussed in Sec. 2.1; this however does not

Table 1: Comparison of the performance for two classifiers: one using five parameters ($W1$, $W1 - W2$, $R - W1$, $B - R$, $w1\text{mag}13$) and the other adding $W3$ as the sixth parameter. TA = total accuracy; c = completeness, and p = purity, all calculated as a weighted arithmetic mean for all five $W1$ bins.

	5D classifier		6D classifier	
	c [%]	p [%]	c [%]	p [%]
galaxies	90.3	89.9	96.8	96.7
quasars	95.1	92.2	98.1	98.6
stars	90.0	88.5	96.9	98.1
TA	91.8 %		97.3 %	

prevent very low signal-to-noise $W3$ measurements (dominating the sample) from introducing possible confusion.

The results for both classifiers are summarized in Table 1. The accuracy, completeness, and purity for both cases are very high. The contamination levels rarely exceed 10%, and 5% in case of 5D and 6D classifier, respectively. The 6D classifier clearly provides better results in all the calculated metrics, which shows that the availability of the $W3$ band allows for (possibly considerable) improvement in the classification. However, the low detection rate in this band (only 30% of our sources have $w3\text{snr} > 2$), and large variations in sensitivity on the sky⁴ mean that using this band could introduce biases into the final catalogue. Based on these considerations, together with the fact that each new classification parameter extends computation time, we decided not to use the $W3$ passband for the final classification.

4.2. General performance of the classifier

To quantify the general performance of the set of five classifiers tuned for different $W1$ magnitude bins, we have analysed the final results (merged output catalogues from different $W1$ bins) of the self-check and the test sample. As the test sample we randomly chose 5,000 galaxies from the same WISE \times SCOS \times SDSS catalogue, independent from the training sample. The total accuracy, calculated over the galaxy test sample, was equal to 92.5%. It was not possible to perform the same analysis for stars and quasars, as for the brightest and faintest bins, all of them were used to build the training sample.

4.2.1. Dependence on the $W1$ magnitude

Having determined the total accuracy of the 5D classifier, we have investigated its performance further, starting with the dependence on the $W1$ magnitude for the three classes. The results are illustrated in Fig. 4 for the self-check (left panel) and test (right panel, only for galaxies) samples. In general the accuracies retain very high levels, of the order of 90%, but there is significant deterioration in classification quality for faint galaxies and stars. This is related to the fact that beyond $W1 \gtrsim 15.5$ the training set contains very few galaxies and stars. The misclassification of galaxies happens mainly for objects with $W1 > 15$ mag, and in most cases, true galaxies are misclassified as stars. The accuracy for galaxies calculated for the test sample has the same dependence on $W1$ magnitude as the one derived from the self check.

⁴ See e.g. http://wise2.ipac.caltech.edu/docs/release/allsky/expsup/sec6_2.html.

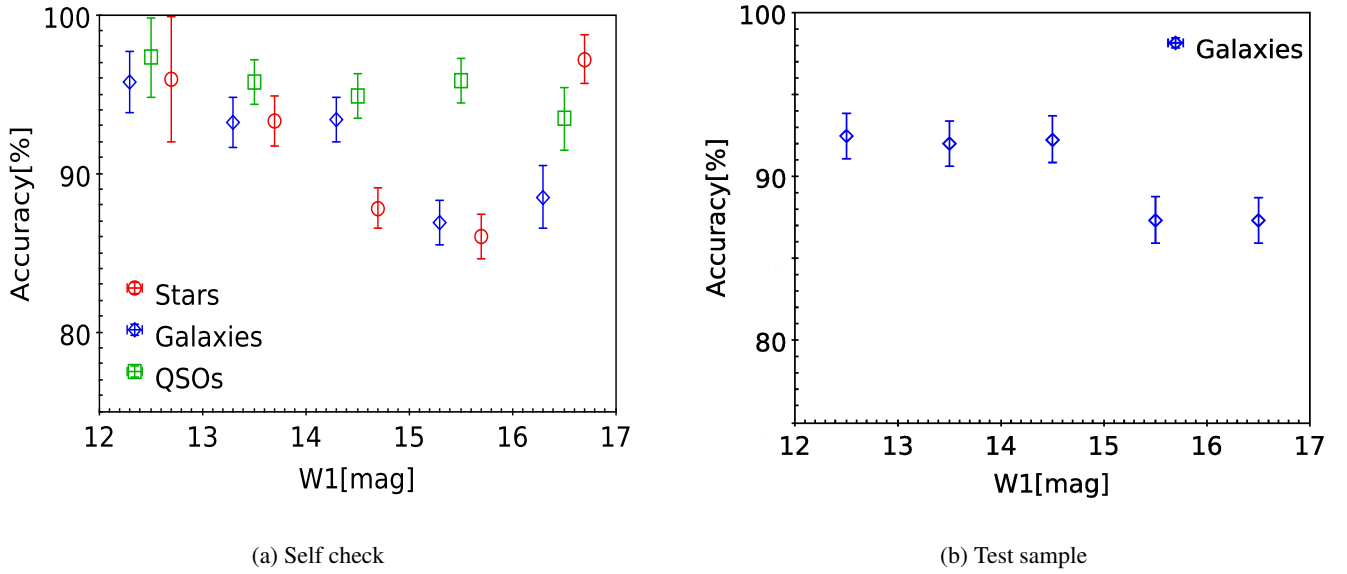


Fig. 4: Accuracy of the 5D classifier as a function of the limiting $W1$ magnitude, for the three types of classified sources, for the self check (*left panel*) and the test sample (*right panel*). Blue diamonds correspond to galaxies, green squares to quasars, and red circles to stars. The points were shifted horizontally for clarity.

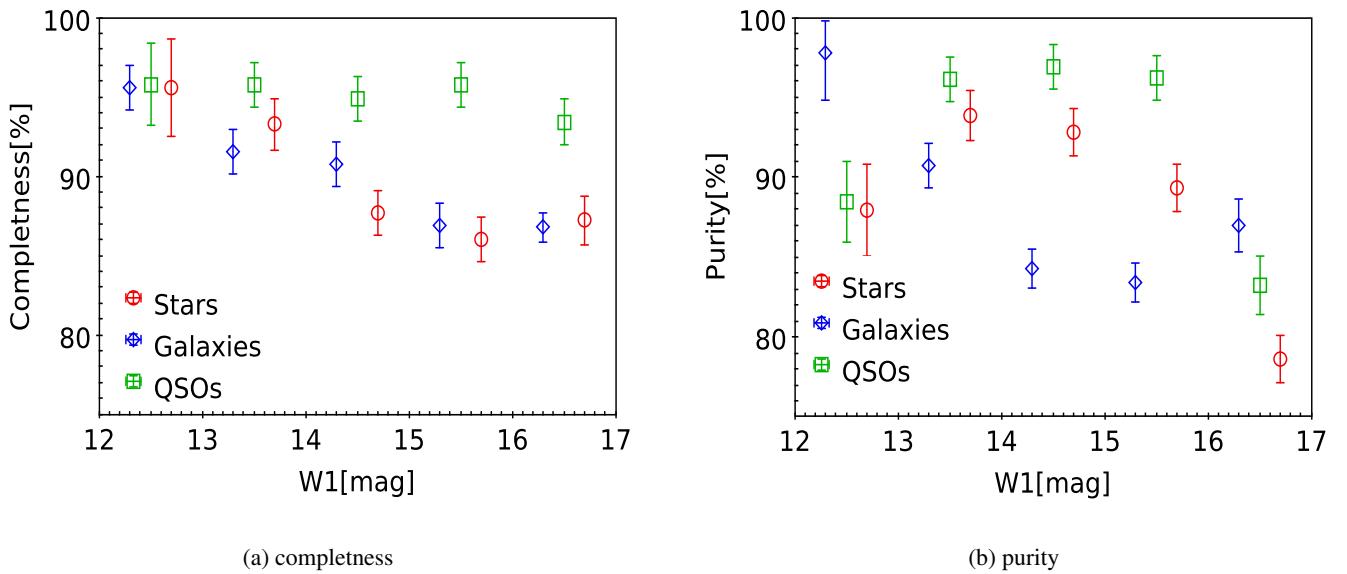


Fig. 5: Completeness and purity for galaxies, stars, and quasars as a function of the $W1$ magnitude for the 5D classifier. These results refer to the self-check.

As we show in Fig. 5a, also the completeness of the galaxy sample decreases with increased $W1$. For galaxies in the $15 \leq W1 < 17$ mag bin, the completeness equals $\sim 87\%$. Such deterioration was expected, as there are much fewer training objects in the galaxy and star samples for the faintest $W1$ bin than in the quasar one.

We have also checked the purity as a function of $W1$ for the sources classified with the 5D classifier. As Fig. 5b shows, it is at similar levels as the completeness, although its dependence on $W1$ is somewhat different. In particular, for all the 3 classes, there is a significant decrease in purity at the faint end. Still, as far as galaxies are concerned (of main interest for the present

analysis), it stays at a reasonable level of $p > 80\%$ in all the bins.

Based on the findings of this Section, we conclude that the 5D classifier is stable and can be safely used for the final classification. In principle, using the self check and test results, we could estimate the main statistics of the final WISE \times SCOS galaxy catalogue. The caveat is however that the SDSS training sample may not be representative enough for the WISE \times SCOS dataset, which can lead to biases in such assessments of the final sample quality.

In the final catalogue we will keep all the sources preselected as in Sec. 2, but – owing to the above considerations – for more sophisticated analyses it might be preferable to remove

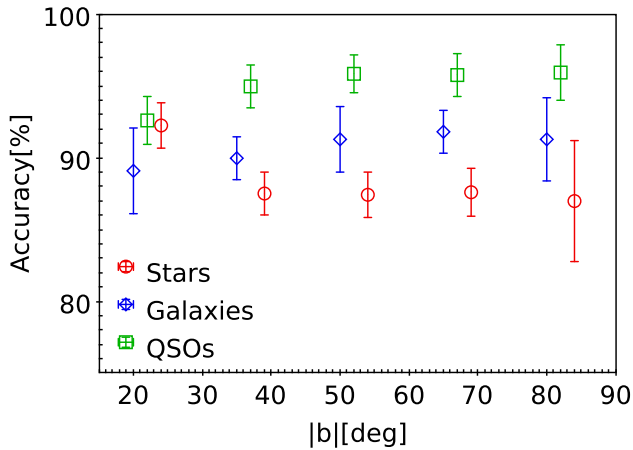


Fig. 6: Accuracy of the 5D classifier as a function of Galactic latitude, with respect to the three classes of sources.

the faintest ones to avoid possible misclassification. Nevertheless, we stress that the classification accuracy for the fainter part of our galaxy sample is still satisfying as it reaches very high levels even for the faintest sources (87% for $15 < W1 < 16$ mag bin, and ~90% for galaxies with $W1 > 16$ mag for the self-check of the 5D classifier, and more than 85% for the galaxy test sample with $W1 > 15$ mag).

4.2.2. Dependence on the Galactic latitude

We also checked how the accuracy of the five classifiers depends on the Galactic latitude, b . We divided the training sample into six 15° -wide bins in $|b|$, and calculated the accuracy for each of the bins. The results are shown in Fig. 6. For the lowest latitude bin of $|b| < 15^\circ$, the training sample contains practically no galaxies nor quasars, it will thus not be used in this test. This also means that to avoid extrapolation, one may need to discard this area from the eventual galaxy catalogue.

5. Results: final galaxy catalogue

Having thoroughly verified the performance of the SVM algorithm on the test data, we applied it to the full WISE \times SCOS sample described in Sec. 2. In order to prepare the final galaxy catalogue based on our automatic classification, we used additional information provided by SVM, namely the probabilities that the sources belong to particular classes. We also checked the catalogue for outliers in magnitude and colour space, and finally we compared it with the one presented in B16 where simple colour cuts were employed for star and quasar removal.

Although the SVM classifier assigns the final discrimination based on discrete classes, it also provides additional information on object's distance from different boundaries, which can be used as a probability for a given source to belong to a particular class. The probability calculated in SVM is given by the formula from Platt (1999) and such an a posteriori probability function was implemented in the SVM kernel by Lin et al. (2007). For classification into more than two source types, the single class probabilities are combined together to estimate final probabilities by the pairwise coupling method (for detailed information see Wu et al. 2003). As our aim is to obtain a pure galaxy sample (with a strong decision value), we decided to take advantage

of the full probability distributions to eliminate sources of unclear classification (located between different classes), instead of using discrete classes only. Initially, the galaxy candidate catalogue output by SVM (i.e. such that $p_{\text{gal}} > p_{\text{star}}$ and $p_{\text{gal}} > p_{\text{QSO}}$) included over 16.8 million sources. As in Kurcz et al. (2016), also here we checked if cuts on source type probabilities could lead to an improvement in quality of the catalogue. Unlike in that analysis, however, in the case of WISE \times SCOS galaxies even a cut of $p_{\text{gal}} > 0.5$ (as well as more aggressive ones) did not lead to an increase in the purity of the sample, while it lowered its completeness. For the subsequent analysis we will thus keep all the sources flagged as galaxies by SVM. We note that the here derived SVM probability values will be made available in the WISE \times SCOS database. This will allow users to apply their own cuts in order to purify the sample (at the expense of its completeness), for instance by putting maximum thresholds on p_{star} and p_{QSO} , or cutting more aggressively on p_{gal} .

The resulting catalogue was examined further for possible outliers in magnitude and colour space. Here we used the WISE \times SCOS \times SDSS data as the calibration, to look for cases of extreme extrapolation from the training data. We found a very small number (only ~1500) of sources that had colours very different from those in the calibration sample. Majority of them are located near the Galactic Plane or by the Magellanic Clouds, where WISE \times SCOS photometry is problematic due to blending. Such areas anyway need to be masked out, using a mask such as the one derived in B16. Application of that mask to the current catalogue leaves 15 million sources, shown in Fig. 7.

5.1. Comparison with Bilicki et al. (2016)

It is interesting to compare the WISE \times SCOS galaxy catalogue derived in this paper with the one presented in B16. The parent sample used in there was the same as in here, but galaxies were separated from stars and quasars through colour cuts. In particular, the star-galaxy separation was done through a position-dependent cut in the $W1 - W2$ colour to accommodate for variations in the stellar locus with the position in the Galaxy. At high Galactic latitudes the cut was $W1 - W2 > 0$, while it was gradually increased at lower latitudes to reach $W1 - W2 > 0.12$ by the Galactic Plane and Bulge; see section 4.2 and appendix of B16 for details. To this, three cuts were added to mitigate stellar contamination and blending: (i) removal of the bright-end of the sample ($W1 < 13.8$), dominated by stars on the one hand, and already sampled extragalactically by the 2MASS Photometric Redshift catalogue (2MPZ, Bilicki et al. 2014) on the other; (ii) a cutout of the Galactic Bulge reaching up to $|b| = 17^\circ$ at $\ell = 0^\circ$; (iii) manual cutouts of the Magellanic Clouds and M31. Finally, quasars and blends thereof were removed by B16 with colour cuts in the $(W1 - W2) - (R - W2)$ plane: anything with $R - W2 > 7.6 - 4(W1 - W2)$ or $W1 - W2 > 0.9$ was discarded. These cuts resulted in a dataset of 21.5 million sources; however, the sample still presented some spurious over- and underdensities in some areas, and an iterative procedure was performed to design the final mask. After the masking, the eventual WISE \times SCOS galaxy catalogue of B16 included 18.7 million sources over 68% of the sky.

A cross-match of the SVM galaxy dataset with the one by B16 gives over 14.8 million common sources, which means that there are almost 2×10^6 objects identified by SVM as galaxies, which had been removed from the B16 sample. However, for this comparison to be meaningful, we should also remove the $W1 < 13.8$ sources from the SVM catalogue, as well as those in the Bulge area, in the same way as in B16. These two cuts

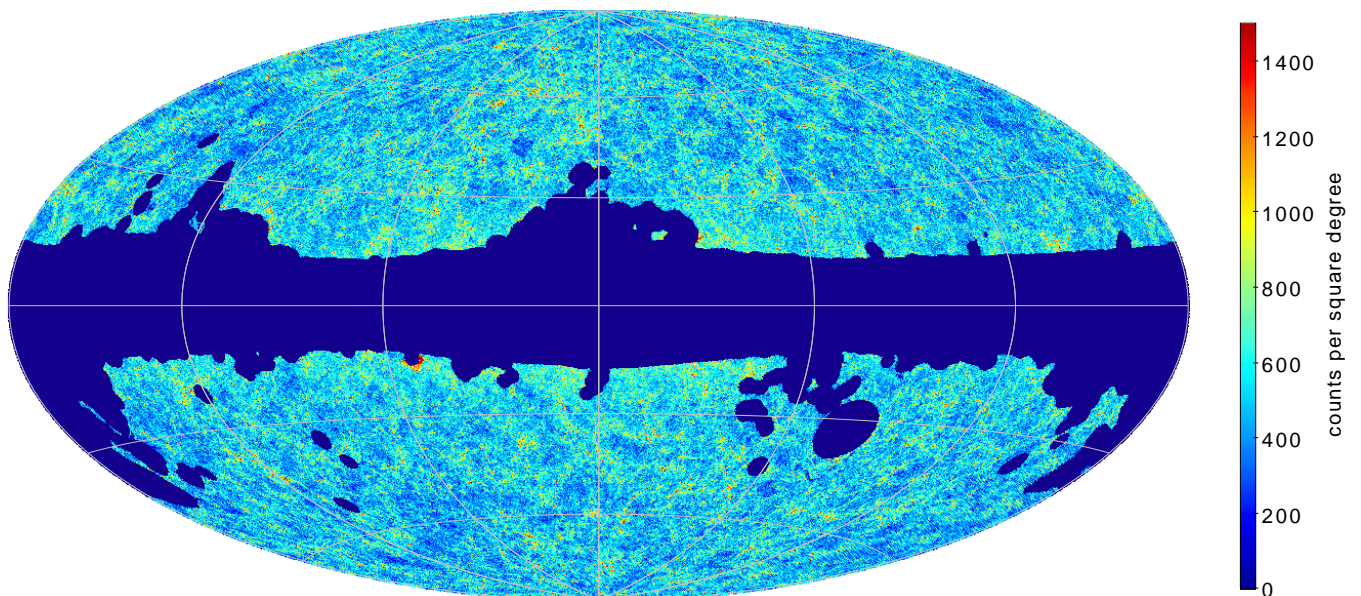


Fig. 7: Aitoff projection of sources identified by SVM as galaxy candidates in the WISE \times SCOS catalogue, after cleanup of low-probability objects and masking (see text for details). This plot shows 15 million objects in Galactic coordinates (with $\ell = 0^\circ$, $b = 0^\circ$ at the centre).

reduce the "in SVM, not in colour-cut" sample to 1.3 million, roughly 8% of the original SVM galaxy dataset. These objects are mostly concentrated at low Galactic latitudes ($|b| < 30^\circ$) and around Magellanic Clouds, i.e. in areas where stellar blending affecting both parent catalogues has a negative impact on the photometry of extracted sources. Practically all of these objects have $W1 - W2 < 0.12$, as one should expect (the upper limit of the B16 adaptive cut), and 1 million of them are outside the B16 mask. In general, the colours of the sources identified by SVM as galaxies but not present in the B16 catalogue are consistent with those of SDSS stars or quasars.

Interestingly, practically no sources identified by B16 as quasars are present in the SVM galaxy catalogue – there are 1300 objects meeting the QSO colour criteria mentioned above found in the SVM dataset. As those colour cuts were calibrated on a comparison of SDSS QSOs and GAMA galaxies, we conclude that our present catalogue is practically free of quasar contamination. This is consistent with the results from the test sets presented in Sec. 4.2.

There are significantly more sources (5.6 million after masking) in the B16 galaxy catalogue which are not present in the SVM one, than the other way round. They are generally distributed over the entire sky, although their surface density increases towards the Galactic Plane. Their $W1 - W2$ colour distribution is bimodal, with one peak at $W1 - W2 \sim 0.1$ and the other at $W1 - W2 \sim 0.5$. The former might indeed be stars which survived the position-dependent cut of B16, but were correctly classified by SVM. The latter are probably starburst/dusty galaxies, which our training sample is less sensitive to, hence they were partly misidentified by the classifier and removed from the SVM dataset; they were however (correctly) kept in the B16 sample.

Finally, a comparison of source counts as a function of Galactic latitude (Fig. 8) suggests that the SVM catalogue is purer than the one by B16, as the rise in the number counts with decreasing absolute latitude is happening at lower $|b|$ in the former than in the latter. However, as B16 estimated that their catalogue was less than 90% complete at $|b| > 30^\circ$ ($|\sin(b)| > 0.5$), and the absolute counts of the present dataset are smaller than

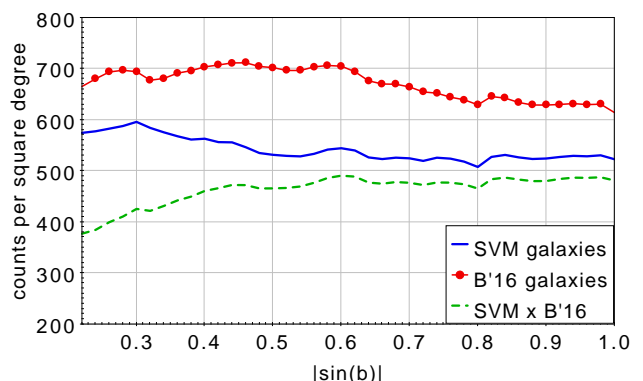


Fig. 8: Number counts, as a function of the sine of Galactic latitude, for three samples of WISE \times SuperCOSMOS galaxies: selected with colour cuts by Bilicki et al. (2016) (red dotted); identified by SVM (present work; blue solid); and common to both datasets (green dashed).

those of the B16 sample even in the Galactic Caps, we conclude that the higher purity of the SVM catalogue comes at a price of its lower completeness.

6. Summary

The WISE \times SCOS galaxy sample is currently the largest in terms of its size and sky coverage at $z \sim 0.2$, giving access to angular scales not accessible with such samples as SDSS, being at the same time much deeper than other ‘all-sky’ datasets, available from IRAS or 2MASS. Here we presented an approach to identifying galaxies in the WISE \times SCOS photometric data which is alternative to the colour cuts applied in Bilicki et al. (2016). By using the support vector machines algorithm, trained and tested on a cross-match of spectroscopic SDSS data with WISE \times SCOS, we identified about 15 million galaxy candidates over 70% of sky. This number is smaller than 18.5 million obtained by B16, mostly because of the higher purity but lower

completeness of the present sample than the colour-selected one. The resulting source probabilities assigned by SVM will be provided in the photometric redshift WISE \times SCOS dataset released together with the B16 publication, available from the Wide Field Astronomy Unit, Institute for Astronomy, Edinburgh at <http://ssa.roe.ac.uk/WISExSCOS.html>.

In the present study we focused on galaxies, as we were using only extended (resolved) sources from SuperCOSMOS. Still, this work could be in principle continued to obtain more general star/galaxy/quasar identification in the full WISE \times SCOS sample. This would however require SCOS point-source photometry to be calibrated all-sky in a similar way as the aperture one (Peacock et al. 2016), which currently is not the case.

Successful machine-learning galaxy identification in WISE \times SCOS shows that a similar approach will be worthwhile for other samples based on WISE, cross-matched with such forthcoming wide-angle datasets as from Pan-STARRS, SkyMapper, or VHS. As far as WISE itself is concerned, first efforts on all-sky star/galaxy/QSO separation in that catalogue are already reported on in Kurcz et al. (2016).

Acknowledgements. We are grateful to John Peacock for his useful comments. Special thanks to Mark Taylor for TOPCAT⁵ (Taylor 2005) and STILTS⁶ (Taylor 2006) software. Some of the results in this paper have been derived using the HEALPix package⁷ (Górski et al. 2005).

This publication makes use of data products from the Wide-field Infrared Survey Explorer, which is a joint project of the University of California, Los Angeles, and the Jet Propulsion Laboratory/California Institute of Technology, and NEOWISE, which is a project of the Jet Propulsion Laboratory/California Institute of Technology. WISE and NEOWISE are funded by the National Aeronautics and Space Administration.

This research has made use of data obtained from the SuperCOSMOS Science Archive, prepared and hosted by the Wide Field Astronomy Unit, Institute for Astronomy, University of Edinburgh, which is funded by the UK Science and Technology Facilities Council.

Funding for SDSS-III has been provided by the Alfred P. Sloan Foundation, the Participating Institutions, the National Science Foundation, and the U.S. Department of Energy Office of Science. The SDSS-III web site is <http://www.sdss3.org/>. SDSS-III is managed by the Astrophysical Research Consortium for the Participating Institutions of the SDSS-III Collaboration including the University of Arizona, the Brazilian Participation Group, Brookhaven National Laboratory, Carnegie Mellon University, University of Florida, the French Participation Group, the German Participation Group, Harvard University, the Instituto de Astrofísica de Canarias, the Michigan State/Notre Dame/JINA Participation Group, Johns Hopkins University, Lawrence Berkeley National Laboratory, Max Planck Institute for Astrophysics, Max Planck Institute for Extraterrestrial Physics, New Mexico State University, New York University, Ohio State University, Pennsylvania State University, University of Portsmouth, Princeton University, the Spanish Participation Group, University of Tokyo, University of Utah, Vanderbilt University, University of Virginia, University of Washington, and Yale University.

MB, KM, AP, AK and MK were supported by the Polish National Science Center under contract #UMO-2012/07/D/ST9/02785. AP, KM and TK were supported by the National Science Centre (grants UMO-2012/07/B/ST9/04425 and UMO-2013/09/D/ST9/04030), the Polish-Swiss Astro Project (co-financed by a grant from Switzerland, through the Swiss Contribution to the enlarged European Union), and the European Associated Laboratory Astrophysics Poland-France HECOLS. MB was supported by the Netherlands Organization for Scientific Research, NWO, through grant number 614.001.451, and through FP7 grant number 279396 from the European Research Council.

References

Alam, S., Albareti, F. D., Allende Prieto, C., et al. 2015, *ApJS*, 219, 12
 Assef, R. J., Stern, D., Kochanek, C. S., et al. 2013, *ApJ*, 772, 26
 Bilicki, M., Jarrett, T. H., Peacock, J. A., Cluver, M. E., & Steward, L. 2014, *ApJS*, 210, 9
 Bilicki, M., Peacock, J., Jarrett, T., et al. 2016, *ApJS*, in press

⁵ <http://www.star.bristol.ac.uk/~mbt/topcat/>

⁶ <http://www.star.bristol.ac.uk/~mbt/stilts/>

⁷ <http://healpix.sourceforge.net/>

Bolton, A. S., Schlegel, D. J., Aubourg, E., et al. 2012, *AJ*, 144, 144
 Brescia, M., Cavaoti, S., & Longo, G. 2015, *MNRAS*, 450, 3893–3903
 Chang, C.-C. & Lin, C.-J. 2011, *ACM Transactions on Intelligent Systems and Technology*, 2, 27:1–27:27, software available at <http://www.csie.ntu.edu.tw/~cjlin/libsvm>
 Cluver, M. E., Jarrett, T. H., Hopkins, A. M., et al. 2014, *ApJ*, 782, 90
 Cristianini, N. & Shawe-Taylor, J. 2000, *An Introduction to Support Vector Machines: And Other Kernel-Based Learning Methods* (Cambridge University Press)
 Cutri, R. M., Wright, E. L., Conrow, T., et al. 2012, Explanatory Supplement to the WISE All-Sky Data Release Products, Tech. rep.
 Cutri, R. M., Wright, E. L., Conrow, T., et al. 2013, Explanatory Supplement to the AllWISE Data Release Products, Tech. rep.
 Ferraro, S., Sherwin, B. D., & Spergel, D. N. 2015, *Phys. Rev. D*, 91, 083533
 Górski, K. M., Hivon, E., Banday, A. J., et al. 2005, *ApJ*, 622, 759–771
 Hambly, N. C., Davenhall, A. C., Irwin, M. J., & MacGillivray, H. T. 2001a, *MNRAS*, 326, 1315–1327
 Hambly, N. C., Irwin, M. J., & MacGillivray, H. T. 2001b, *MNRAS*, 326, 1295–1314
 Hambly, N. C., MacGillivray, H. T., Read, M. A., et al. 2001c, *MNRAS*, 326, 1279–1294
 Han, B., Ding, H.-P., Zhang, Y.-X., & Zhao, Y.-H. 2016, *Research in Astronomy and Astrophysics*, 16, 005
 Huertas-Company, M., Rouan, D., Tasca, L., Soucail, G., & Le Fèvre, O. 2008, *A&A*, 478, 971–980
 Jarrett, T. H., Cluver, M. E., Magoulas, C., et al. 2016, *ApJ*, submitted
 Jarrett, T. H., Cohen, M., Masci, F., et al. 2011, *ApJ*, 735, 112
 Kovács, A. & Szapudi, I. 2015, *MNRAS*, 448, 1305–1313
 Kurcz, A., Bilicki, M., Solarz, A., et al. 2016, *arXiv:1604.04229*
 Lin, H.-T., Lin, C.-J., & Weng, R. C. 2007, *Mach. Learn.*, 68, 267–276
 Manning, C. D., Raghavan, P., & Schütze, H. 2008, *Introduction to Information Retrieval* (New York, NY, USA: Cambridge University Press)
 Marton, G., Tóth, L. V., Paladini, R., et al. 2016, *MNRAS*, 458, 3479
 Malek, K., Solarz, A., Pollo, A., et al. 2013, *A&A*, 557, A16
 Meyer, D. 2001, *R News*, 1, 23–26
 Peacock, J., Hambly, N., Bilicki, M., et al. 2016, *MNRAS*, submitted
 Platt, J. C. 1999, in *ADVANCES IN LARGE MARGIN CLASSIFIERS* (MIT Press), 61–74
 Rahman, M., Ménard, B., & Scranton, R. 2016, *MNRAS*
 Saglia, R. P., Tonry, J. L., Bender, R., et al. 2012, *ApJ*, 746, 128
 Schlafly, E. F. & Finkbeiner, D. P. 2011, *ApJ*, 737, 103
 Schlegel, D. J., Finkbeiner, D. P., & Davis, M. 1998, *ApJ*, 500, 525
 Shawe-Taylor, J. & Cristianini, N. 2004, *Kernel Methods for Pattern Analysis* (Cambridge University Press)
 Skrutskie, M. F., Cutri, R. M., Stiening, R., et al. 2006, *AJ*, 131, 1163–1183
 Solarz, A., Pollo, A., Takeuchi, T. T., et al. 2012, *A&A*, 541, A50
 Soumagnac, M. T., Abdalla, F. B., Lahav, O., et al. 2015, *MNRAS*, 450, 666–680
 Stern, D., Assef, R. J., Benford, D. J., et al. 2012, *ApJ*, 753, 30
 Stoughton, C., Lupton, R. H., Bernardi, M., et al. 2002, *AJ*, 123, 485–548
 Taylor, M. B. 2005, in *Astronomical Society of the Pacific Conference Series*, Vol. 347, *Astronomical Data Analysis Software and Systems XIV*, ed. P. Shopbell, M. Britton, & R. Ebert, 29
 Taylor, M. B. 2006, in *Astronomical Society of the Pacific Conference Series*, Vol. 351, *Astronomical Data Analysis Software and Systems XV*, ed. C. Gabriel, C. Arviset, D. Ponz, & S. Enrique, 666
 Vasconcellos, E. C., de Carvalho, R. R., Gal, R. R., et al. 2011, *AJ*, 141, 189
 Woźniak, P. R., Williams, S. J., Vestrand, W. T., & Gupta, V. 2004, *AJ*, 128, 2965–2976
 Wright, E. L., Eisenhardt, P. R. M., Mainzer, A. K., et al. 2010, *AJ*, 140, 1868–1881
 Wu, T.-f., Lin, C.-J., & Weng, R. C. 2003, *Journal of Machine Learning Research*, 5, 975–1005
 Yan, L., Donoso, E., Tsai, C.-W., et al. 2013, *AJ*, 145, 55